A Temporal Bottleneck in the Language Comprehension Network

Laurianne Vagharchakian, Ghislaine Dehaene-Lambertz, Christophe Pallier, Stanislas Dehaene

Behavioral/Systems/Cognitive

A Temporal Bottleneck in the Language Comprehension Network

Laurianne Vagharchakian,[1,2,3] Ghislaine Dehaene-Lambertz,[1,2,3] Christophe Pallier,[1,2,3] and Stanislas Dehaene[1,2,3,4]

[1]Institut National de la Santé et de la Recherche Médicale, Cognitive Neuroimaging Unit, F91191 Gif-sur-Yvette, France, [2]Commissariat à L'Énergie Atomique et aux Énergies Alternatives, NeuroSpin Center, F91191 Gif-sur-Yvette, France, [3]Université Paris XI, 91405 Orsay, France, and [4]Collège de France, 75231 Paris, France

Humans can understand spoken or written sentences presented at extremely fast rates of ~400 wpm, far exceeding the normal speech rate (~150 wpm). How does the brain cope with speeded language? And what processing bottlenecks eventually make language incomprehensible above a certain presentation rate? We used time-resolved fMRI to probe the brain responses to spoken and written sentences presented at five compression rates, ranging from intelligible (60–100% of the natural duration) to challenging (40%) and unintelligible (20%). The results show that cortical areas differ sharply in their activation speed and amplitude. In modality-specific sensory areas, activation varies linearly with stimulus duration. However, a large modality-independent left-hemispheric language network, including the inferior frontal gyrus (pars orbitalis and triangularis) and the superior temporal sulcus, shows a remarkably time-invariant response, followed by a sudden collapse for unintelligible stimuli. Finally, linear and nonlinear responses, reflecting a greater effort as compression increases, are seen at various prefrontal and parietal sites. We show that these profiles fit with a simple model according to which the higher stages of language processing operate at a fixed speed and thus impose a temporal bottleneck on sentence comprehension. At presentation rates faster than this internal processing speed, incoming words must be buffered, and intelligibility vanishes when buffer storage and retrieval operations are saturated. Based on their temporal and amplitude profiles, buffer regions can be identified with the left inferior frontal/anterior insula, precentral cortex, and mesial frontal cortex.

Introduction

We typically speak at a rate of ~130–190 words per minute (wpm) (Reynolds and Givens, 2001). However, surprisingly, the language comprehension system can sustain much faster presentation rates. Using digital compression, speech can be accelerated up to ~40% of its original duration and remain largely comprehensible (Chodorow, 1979; Mehler et al., 1993; Dupoux and Green, 1997; Pallier et al., 1998; Sebastian-Galles et al., 2000). Furthermore, during reading, expert readers typically attain 250–300 wpm, and reading speed can be doubled or tripled by removing the need for eye movements (Rubin and Turano, 1992).

Here, we use functional magnetic resonance imaging (fMRI) to investigate how the language system copes with fast presentation rates. Although fMRI has a low temporal resolution compared with electrophysiological methods, it can detect activation delays and duration changes of ~200 ms (Menon et al., 1998; Sigman et al., 2007; Sigman and Dehaene, 2008). In response to a single sentence, language areas show a systematic temporal organization, with increasingly delayed responses as one moves either posterior or anterior to primary auditory cortex, the slowest response being observed in left inferior frontal gyrus (Dehaene-Lambertz et al., 2006; Brauer et al., 2008; Pallier et al., 2011). This temporal gradient of activation might result from a succession of processes that integrate over increasingly larger, and possibly more abstract, linguistic units, therefore requiring longer processing time or more sustained activity (see also Hasson et al., 2008; Lerner et al., 2011; Brennan et al., 2012).

Here, we evaluated how this temporal organization varies with presentation rate. Unlike previous fMRI studies of speech compression that used block designs (Poldrack et al., 2001; Peelle et al., 2004, 2010; Adank and Devlin, 2010), we used a slow event-related design to measure the fMRI response to a single sentence, thus allowing us to determine whether cortical processing speed, indexed by the phase of the fMRI response, accelerates when the stimulus is speeded; which regions show a sudden collapse of activation in parallel to the sudden loss of intelligibility at fast presentation rates; and how these effects differ for spoken and written language.

Our main goal was to clarify the mechanisms that eventually limit the intelligibility of compressed speech. One possibility is a sensory bottleneck; at high compression rates, incoming visual or auditory information would be degraded beyond recognition due to its short presentation time or to masking by the next stimulus. Another possibility is a saturation of a postperceptual processing stage. The integration of successive words into a sentential structure may create a processing bottleneck, analogous to attentional blink and psychological refractory period phenomena (Pashler,

Received Nov. 11, 2011; revised March 20, 2012; accepted April 17, 2012.

Author contributions: L.V., G.D.-L., and S.D. designed research; L.V. and G.D.-L. performed research; L.V., G.D.-L., C.P., and S.D. analyzed data; L.V., G.D.-L., C.P., and S.D. wrote the paper.

This work was supported by the McDonnell Foundation, Agence Nationale de la Recherche (France), and Ecole des Neurosciences de Paris-Neuropole de Recherche Francilien.

The authors declare no competing financial interests.

Correspondence should be addressed to Ghislaine Dehaene-Lambertz, INSERM U992, CEA/SAC/DSV/DRM/NeuroSpin, Bât 145, Point Courrier 156, 91191 Gif-sur-Yvette, France. E-mail: ghislaine.dehaene@cea.fr.

DOI:10.1523/JNEUROSCI.5685-11.2012

 0270-6474/12/329089-14$15.00/0

1984; Raymond et al., 1992; Sigman and Dehaene, 2008), thus delaying the processing of subsequent incoming words and requiring their temporary storage in a buffer. The collapse of intelligibility at fast rates would be due to the saturation of this buffer. Within this framework, the responses of different brain areas to speeded stimuli could provide insight into the brain architecture for language processing.

Materials and Methods

Participants

Participants were 16 young native French speakers (14 males; mean age, 22 years; SD, 2.6 years) with no history of oral or written language impairment, neurological disease, or psychiatric disease. All were right-handed and had normal or corrected-to-normal vision and no hearing deficits. All participants gave their written informed consent, and the study was approved by the local ethics committee.

Stimuli

A set of 264 sentences was constructed using the following criteria: each sentence was plausible, nonambiguous, and right branching; each consisted of 12 words and of 16 or 17 syllables. The number of letters per word varied from 1 to 13 (mean, 4.4 letters; SD, 2.2 letters; third quartile, 6 letters).

The sentences were digitally recorded at 22.05 kHz in a quiet room by a female speaker trained to produce the sentences at a constant speed while keeping a natural intonation. Sentences had a mean total duration of 2.8 s (SD, 0.14 s), corresponding to 5.9 syllables/s or ~256 wpm—a fast but easily intelligible rate. The sentences were then compressed to 20, 40, 60, or 80% of their original duration using the PSOLA algorithm implemented in the Praat software (www.praat.org). As a partial control for the effects of digital compression, we also recorded the same sentences at a higher speed of pronunciation (mean duration, 2.06 s; SD, 0.12 s; 8 syllables/s or 291 wpm). These faster sentences were then compressed to 54% of their original duration, yielding a second set of stimuli with the same duration as the natural sentences compressed at 40% (duration, 1.12 s). We reasoned that if the compression algorithm was efficient at simulating natural increases in elocution rate, then performance should only be determined by final stimulus duration rather than by the original recording speed or by the compression rate. This claim can be assessed by comparing the behavioral and fMRI results for these two sets of recordings (natural elocution speed compressed to 40% vs speeded elocution compressed to 54%, respectively, labeled 40%N and 40%S).

The audio stimuli were delivered through MRI-compatible headphones (MR confon), and the volume was adjusted for each participant to a comfortable hearing level. Visual stimuli were viewed through a mirror and were projected one word at a time in rapid serial visual presentation (RSVP) at the center of a translucent screen using a 60 Hz video projector. The duration of presentation of written sentences was set to match that of the spoken sentences. Thus, the target duration of each written word was, respectively, 46, 93, 140, 186, 233 ms, corresponding to average sentence durations of 0.56, 1.12, 1.68, 2.24, and 2.80 s for the five compression rates.

RSVP was adopted here because of the strict control that it allows on sentence presentation duration. It should be noted, however, that RSVP only partially mimics the processes at work in normal reading because progressive and regressive eye movements are prevented, short grammatical words cannot be skipped, etc (for discussion, see Just et al., 1982). However, note that these caveats do not apply to the auditory compressed-speech condition, and we primarily focused here on the parallels between the auditory and visual modalities.

The stimuli were displayed using custom software written in Python, which adjusted each individual word presentation duration to the nearest integer multiple of the refresh cycle of the projector (16.7 ms) to ensure an accurate total sentence duration. Words were presented in lowercase Arial font (white characters on a black background) and subtended 0.62° of visual angle vertically and 0.35°–4.84° horizontally (mean, 1.65°). The screen was empty during the intersentence interval.

Procedure

Each participant was scanned in four fMRI runs, two with spoken sentences and two with written sentences. The order was interleaved and alternated between participants. A randomly chosen sentence was presented every 12 s in a slow event-related design. None of the sentences were repeated within a given subject. Because adaptation to compressed sentences is an essential parameter affecting their intelligibility (Dupoux and Green, 1997), sentences were presented in miniblocks of 12 sentences, each with the same fixed compression factor. Compression factors were randomly ordered within each session. The first two sentences of each miniblock were considered as an adaptation period and were therefore modeled as a separate condition in Statistical Parametric Mapping (SPM) software (Wellcome Department of Cognitive Neurology, London, UK) analyses, whose results are not presented here.

Each visual run consisted of five miniblocks, one for each compression factor (20, 40, 60, 80, 100%). For the auditory sessions, there was one additional miniblock, corresponding to the speeded recording (20, 40N, 40S, 60, 80, 100%). Each participant was exposed to a total of 264 different sentences (120 in the visual modality and 144 in the auditory modality).

Our general aim was to study the activation of language networks in the course of normal sentence comprehension while minimizing the contribution of working memory, error detection, repair, and other metacognitive processes (for a similar approach, see Tyler and Marslen-Wilson, 2008; Pallier et al., 2011). Therefore, participants were merely asked to attend to the meaning of each sentence and, once it ended, to rate its intelligibility on a scale from 1 (the sentence was not understood at all) to 4 (the sentence was perfectly understood). Participants were instructed to respond after the end of each sentence using a four-key response box. All participants answered with their right hand. For half the participants, the index finger corresponded to 1 and the small finger to 4. This assignment was reversed for the other half of the participants. Participants were instructed to focus on the accuracy of their judgment rather than speed.

Before entering the scanner, the participants were familiarized with the task using a training set of 30 stimuli (three sentences at each compression factor in each modality). Training sentences were drawn from a set of 66 sentences that were not presented during scanning.

Image acquisition and analysis

Functional images were acquired on a 3 T MR scanner (Tim Trio; Siemens) as T2*-weighted echoplanar images (TR = 1.6 s, TE = 30 ms, matrix = 64 × 64, FOV = 256 mm, voxel size = 4 × 4 × 4 mm, number of slices = 30, mode GRAPPA with an accelerator factor of 2). For the anatomical images, a 3-D gradient-echo sequence (TI = 900 ms, TE = 2.98 ms, TR = 2.3 s, voxel size = 1 × 1 × 1.1 mm, FOV = 256 mm) was used. Data were processed with SPM5 (http://www.fil.ion.ucl.ac.uk/spm/software/spm5). Functional images were realigned to the first image in the series and coregistered to the individual anatomy. Anatomical images were normalized to the Montreal Neurological Institute space, and the normalization parameters were applied to the functional images, which were finally smoothed with a 5 mm^3 Gaussian kernel.

Main SPM model: effects of modality and compression. At the single-subject level, a linear model was generated by entering, for each visual run, 20 regressors corresponding to five compression factors, times two sentence types (initial two training sentences vs next 10 testing sentences), times two hemodynamic profiles [standard hemodynamic response function (HRF) and its temporal derivative] plus six regressors of noninterest corresponding to the movement parameters. Similarly, each auditory run was modeled by 24 regressors because there were six conditions of compression plus the movement parameters.

Importantly, event-related responses were modeled by specifying the same duration for all conditions, which was the median of all stimuli (2.81 s), and then convolving with the standard HRF and its derivative. This choice was made so that the different compression rates were modeled by the same HRF profiles in SPM, thus allowing meaningful statistical comparisons of the β weights obtained in the different conditions of sentence compression to be made (for instance, to detect a linear increase in activation with stimulus duration). If we had used a different temporal

profile for each compression rate, such comparisons would be meaningless. This point is problematic for studies that modeled sentence duration into the stipulated neural profile of activation before convolution with the HRF (Adank and Devlin, 2010); this choice surreptitiously amounts to assuming a linear dependency of brain activity with duration and only allows the experimenters to discover brain areas that deviate from this ideal pattern. Other studies do not describe how they addressed this issue (Peelle et al., 2004, 2010) or introduce confounds in their block design by having more sentences per unit of time in blocks with faster compression rates (Poldrack et al., 2001).

The contrast images from each participant for activation during sentence presentation (relative to the implicit intersentence rest period) were then smoothed with an 8 mm Gaussian kernel and entered into a group-level ANOVA model with modality and compression rate as within-subject factors (and one variable of noninterest for each subject).

We designed contrasts to maximally separate brain areas with distinct profiles of response to compression. Previous publications (Binder et al., 1994; Dhankhar et al., 1997; Buchel et al., 1998; Poldrack et al., 2001; Peelle et al., 2004) and pilot analyses indicated that distinct fMRI profiles could be identified: a linear activation with sentence duration (increasing or decreasing); a step function, i.e., a constant activation collapsing suddenly at the shortest duration (similar to behavioral reports of intelligibility); and a quadratic function, i.e., showing a peak of activation at intermediate durations. One difficulty is that these profiles are nonorthogonal (e.g., there are strong correlations between the linear and step functions and between the step and quadratic functions). Thus, we used combinations of these contrasts, plus inclusive or exclusive masking, to parse brain activations in such a manner that each region would appear only in one type of analysis, as follows. (1) Regions showing a linear increase with stimulation duration were identified using a standard linear contrast over the five conditions of compression 20–100% [−2 −1 0 1 2], masked inclusively by a linear contrast over the range 40–100% [0 −3 −1 1 3]. The latter contrast was needed to ensure linearity over the entire range of compression rates and exclude regions that collapsed only for the most compressed sentences (20% compression). (2) Regions in which activation showed a collapse at 20% compression rate but remained approximately constant at longer durations [−4 1 1 1 1]. This contrast was exclusively masked by [0 3 1 −1 −3] and [0 −3 −1 1 3], thus eliminating voxels that showed a significant linear increase or decrease over the range of 40–100% compression rates. (3) Regions showing a maximum of activity for intermediate durations were identified using a standard inverse quadratic contrast across conditions [−2 1 2 1 −2], masked inclusively by [0 3 1 −1 −3] to exclude regions with the "collapse" profile. (4) Finally, regions showing a linear decrease of activity with duration [2 1 0 −1 −2]. This analysis was confined to regions not showing any quadratic responses (exclusive masking by [−2 1 2 1 −2] and by [2 −1 −2 −1 2]).

Unless otherwise reported, all effects passed a voxelwise threshold of $p < 0.05$ corrected using the False Discovery Rate (FDR) method. All mask constraints were thresholded at voxel $p < 0.001$, uncorrected. Each contrast was first tested globally across the visual (V) and auditory (A) modalities of sentence presentation (V + A). As a second step, we tested for a significant interaction with modality (V > A or A > V). In the latter case, the images were masked inclusively by the corresponding contrast within the appropriate modality (V and A, respectively) to ensure that the interaction was indeed due to the appropriate profile of activation within this modality and not to the presence of the opposite profile in the other modality.

We verified that these four profiles of activation, in one modality or in both, accounted for virtually all the task-related regions (i.e., 95.70% of the voxels identified by an overall F test testing for any effect of the compression factor, in either modality, with a threshold of $p < 0.001$ uncorrected, were present in one of the above contrasts).

To ensure that SPM contrasts were identical across the visual and auditory modalities, the 40%S condition, which was unique to the auditory modality, was not included in these contrasts. However, its results were included as a separate condition in the data plots presented as figures. SPM contrasts verified that there was no significant difference between the conditions 40%N and 40%S.

Plots of the time course of the BOLD signal were generated using the MarsBaR toolbox (http://marsbar.sourceforge.net/), which averages the amplitudes across all the voxels in a given region of interest (ROI) and experimental condition. ROIs were defined here as spheres of 10 mm radius centered on the peaks identified by the main SPM analysis (Table 1).

Effect of intelligibility. A distinct general linear model was used to study the cerebral correlates of fluctuations in sentence intelligibility at a fixed compression level. This analysis was restricted to the 40% compression conditions, where intelligibility was most variable. The above first-level individual-subject model was modified by adding the self-reported intelligibility of each sentence as a modulator of BOLD activation, separately for the visual 40% and auditory 40%N and 40%S conditions. Then, a second-level group SPM model was formed with a contrast pooling across these three regressors and, thus, testing for an overall effect of intelligibility across the two modalities.

Phase analysis. To estimate the phase of the event-related BOLD response, an additional first-level model was created using Fourier (sine/cosine) basis functions rather than the standard HRF. This amounts to convolving the indicator variables of each condition of interest (20 or 24 variables for the visual and auditory modalities respectively), with a single cycle of a sine and a cosine waveform with a period equal to the stimulus onset asynchrony (12 s). As in previous models, the six movement variables of noninterest were also included in the design matrix. After estimation of this model within each subject, the mean weights of the sines and cosines for a given condition were extracted within spherical ROIs using MarsBar, as described above. To compute the phase within an ROI, the ratio of these mean regression weights was then transformed with the inverse tangent function to yield a phase between 0 and 2π. Plots of the average phase across participants were generated using circular mean and SE functions. Phases were multiplied by the stimulation period (12 s) and divided by 2π to yield a phase lag of the BOLD response, expressed in seconds. ANOVAs were used to probe the existence of significant phase differences between regions and conditions. This statistical approach can only be considered approximate, as the phases are distributed on a circular scale (0–12 s) rather than a linear scale appropriate for t and F statistics. However, this approximation is appropriate here because we only analyzed regions that showed a classical fMRI activation profile and therefore whose response phase was predominantly distributed in a narrow time window surrounding the classical HRF latency of 3–8 s. Thus, the circularity of the phase space did not contaminate our statistics. As a complementary nonparametric approach, we also tested the presence of a significant increase in fMRI phase with sentence duration using a permutation test. On 1000 runs, the condition labels were randomly permuted within each subject, and the circular group means by condition were recomputed, thus yielding a new slope relating observed phase to sentence duration. The proportion of permuted datasets in which the slope was larger than the one observed in the actual data is the p value for the permutation test.

Results

Behavior

As shown in Figure 1, intelligibility varied with the speed of sentence presentation, which ranged from the natural speech rate (conventionally referred to as a compression factor of 100%, corresponding to 233 ms/word) to compressed sentences (80, 60, 40, or 20 of the original duration; respectively 186, 140, 93, 46 ms/word). Intelligibility ratings were maximal for the normal sentences, showed little or no decrease as the compression factor went from 100 to 60%, and then dropped quite suddenly to the minimum level for the fastest sentences. These observations were confirmed by a two-factor, repeated-measures ANOVA on the mean intelligibility, with modality and compression factor as within-subject variables. A significant main effect was found for the compression ratio ($F_{(4,60)} = 404$; $p < 10^{-15}$). The main effect of modality was not significant ($F_{(1,15)} = 1.9$; $p < 0.2$), but a significant interaction of modality and compression factor

Table 1. Coordinates of significant activation peaks for the three contrasts

	Auditory					Visual					Main effect				Interactions	
	MNI coordinates					MNI coordinates					MNI coordinates			z Score	z Score	
Brain area	x	y	z	Cluster size	z Score	x	y	z	Cluster size	z Score	x	y	z	(A + V)	A-V	V − A
(A) Linear with duration																
L Heschl's gyrus	−48	−20	4	195	>8*	—	—	—	—	—	−52	−24	4	10.4*	>8*	—
R Heschl's gyrus	56	−16	4	299	>8*	—	—	—	—	—	56	−16	4	10.8*	>8*	—
L inferior occipital gyrus	—	—	—	—	—	−24	−96	−8	42	>8*	−24	−96	−8	6.20*	—	7.38*
R inferior occipital gyrus	—	—	—	—	—	24	−96	−8	84	10.5*	24	−96	−8	5.29*	—	6.19*
(B) Collapse for shortest																
L aSTS	−52	−8	−8	482	>8*	−56	−4	−16	85	5.49*	−52	−8	−12	>8*	—	—
L pSTS	−48	−36	4	405	7.69*	−48	−48	12	139	6.41*	−48	−48	12	>8*	—	—
L mSTS	−64	−24	0	405	7.72*	—	—	—	—	—	−64	−24	−4	>8*	3.22	—
R aSTS	48	−20	−4	275	7.74*	56	0	−16	12	3.76	56	0	−12	>8*	4.34	—
L inferior	−52	32	−4	73	5.23	—	—	—	—	—	−52	32	0	5.60*	—	—
frontal gyrus	−48	16	24	73	4.36	−44	12	24	33	4.28	−44	16	24	5.73*	—	—
	−32	32	−12	13	4.18	—	—	—	—	—	−36	32	−12	4.45	—	—
Medial frontal	0	56	−12	19	3.90	—	—	—	—	—	0	56	−12	4.50	—	—
L precentral	—	—	—	—	—	−44	0	52	53	5.23	−48	0	52	4.74	—	—
L inferior occipital gyrus	—	—	—	—	—	−28	−92	0	151	5.36*	−28	−92	0	4.04	—	4.18
R occipito-temporal gyrus	—	—	—	—	—	44	−68	−4	104	5.07*	—	—	—	—	—	—
R mid occipital gyrus	—	—	—	—	—	40	−92	0	104	4.71	—	—	—	—	—	—
L pre-SMA	—	—	—	—	—	−4	8	60	19	4.50	−8	8	56	4.77	—	—
(C) Maximum for intermediate																
L pre-SMA/ACC	−4	20	52	19	3.97	−4	20	48	163	5.28*	−4	20	52	6.26*	—	—
L anterior insula	−28	28	4	17	4.26	−32	24	0	91	5.22*	−32	24	4	5.94*	—	—
R anterior insula	28	28	0	14	4.21	32	24	0	80	5.35*	28	24	0	6.27*	—	—
L precentral	—	—	—	—	—	−24	0	52	24	3.75	−24	−8	56	3.89*	—	—

The three contrasts are as follows: A, Sensory profile: regions showing a linear increase in activation with stimulus duration (contrast [−2 −1 0 1 2] across the five compression factors, masked inclusively by [0 −3 −1 1 3]; see Materials and Methods). B, Post-bottleneck profile: regions showing a sudden collapse in activation at the shortest duration (contrast [−4 1 1 1 1], masked exclusively with the two contrasts [0 3 1 −1 −3] and [0 −3 −1 1 3]). C, Buffer profile: regions showing an inverse quadratic response as a function of stimulus duration (contrast [−2 1 2 1 −2] masked inclusively by [0 3 1 −1 −3]). Left and middle columns report separate tests for the auditory and the visual conditions, respectively, while the "main effect" column collapses across these two conditions. Finally, the "interactions" column reports the *z* score at the peak of the main effect, of the interaction of each of the above contrasts with modality, evaluated as the difference of the auditory and visual contrasts (Table 2 provides a full report of significant peaks for these interaction terms). The threshold was voxelwise $p < 0.05$, FDR corrected, and only clusters with more than 10 voxels are reported. Asterisks indicate clusters that also reached significance by cluster size ($p < 0.05$, corrected across the whole brain volume). The voxel size was 4 * 4 * 4 mm. mSTS, Middle superior temporal sulcus.

($F_{(4,60)} = 8.2; p < 10^{-4}$) reflected the fact that comprehension collapsed more continuously for visual than for auditory sentences (Fig. 1). Indeed, comparisons between modalities at each compression level showed that intelligibility in the visual modality already decreased at 80% compression, while intelligibility in the auditory domain was still preserved ($t_{(15)} = 3.32; p = 0.004$). This difference between modalities was even more pronounced at 60% compression ($t_{(15)} = 4.19; p = 8.10^{-4}$).

A similar ANOVA on reaction times (RTs), measured from sentence ending, showed that participants were faster for auditory sentences than for visual ones ($F_{(1,15)} = 5.42; p < 0.04$) and that the RT depended on the compression ratio ($F_{(4,60)} = 29.15; p < 10^{-12}$), with no significant interaction between the two factors ($F_{(4,60)} = 2.06; p = 0.1$). The main effect of compression ratio was due to a slowing down for the 40% condition, where participants were significantly slower than in the other conditions ($t_{(15)} = -9.73; p < 8.10^{-11}$).

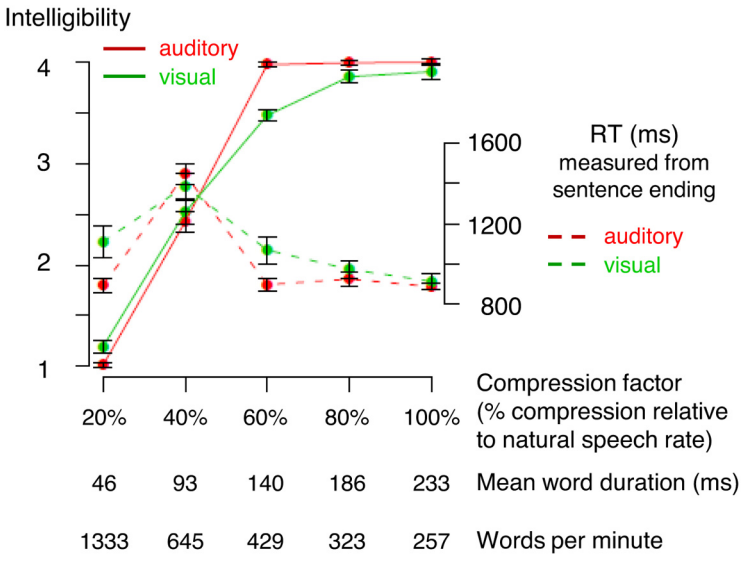

Figure 1. Behavioral results during fMRI acquisition. Intelligibility score (left axis and solid line) and reaction time measured from the end of the sentence (right axis and dotted line) are plotted as a function of the compression factor (for convenience, this value is also converted to mean word duration and word rate). Intelligibility was subjectively rated using a four-button press, specified as follows: 1, nothing understood; 2, weakly understood; 3, mostly understood; 4, completely understood. Each point was averaged over 20 items per conditions and per subject (bars indicate 1 SE). Red, Auditory modality; Green, visual modality.

No behavioral difference was noted between the two auditory conditions 40%N and 40%S ($t_{(15)} < 1$ for intelligibility and reaction time). The fact that these two conditions had the same final duration and differed only in their relative proportions of digital compression versus initial natural speech rate suggests that the computer algorithm for speech compression was efficient at simulating natural changes in elocution rate and extending them to

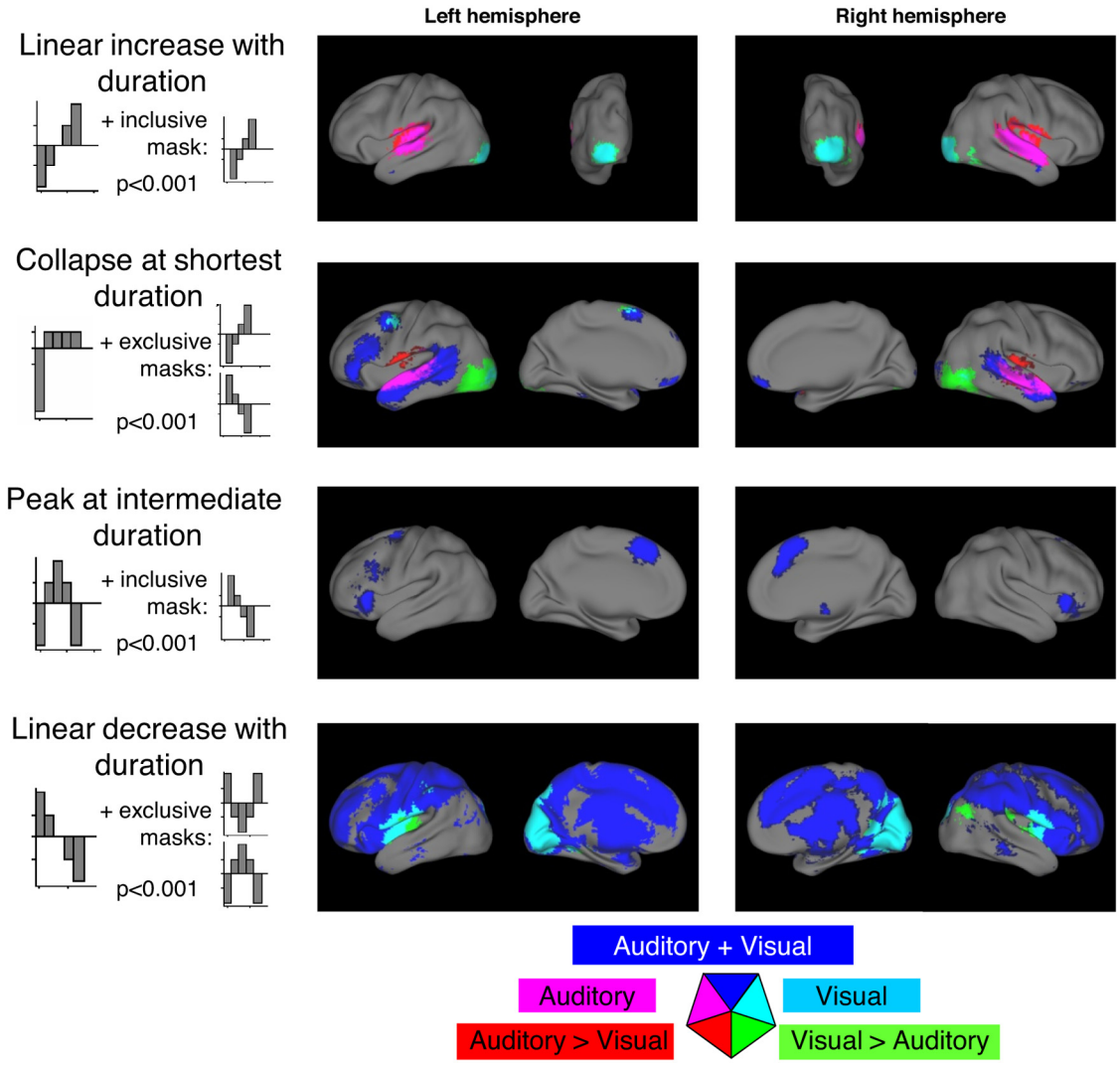

Figure 2. Classification of regions exhibiting a significant modulation of activation amplitude with compression rate ($p < 0.001$). Blue, Main effect across both written and spoken sentences. Green and red, Interaction terms indicating a significantly greater effect for written sentences (green) or for spoken sentences (red). First row, Lateral and posterior maps showing areas with a linear increase of activation as a function of the five compression factors (20, 40, 60, 80, or 100% of natural speech rate: linear contrast [−2 −1 0 1 2] inclusively masked by [0 −3 −1 1 3]). Second row, Lateral and medial maps showing areas with a collapse of activation at the shortest stimulus duration (nonlinear contrast [−4 1 1 1 1] exclusively masked by [0 3 1 −1 −3] and [0 −3 −1 1 3]). Third row, Lateral and medial maps showing areas with a maximum of activation for intermediate compression factors (quadratic contrast [−2 1 2 1 −2] inclusively masked by [0 3 1 −1 −3]). Fourth row, Lateral and medial maps showing areas with a linear increase in activation as the compression factor gets shorter (linear contrast [2 1 0 −1 −2] exclusively masked by [−2 1 2 1 −2] and by [2 −1 −2 −1 2]).

compression factors beyond those producible by a natural speaker.

fMRI amplitude variations with stimulus duration

fMRI activation increasing linearly with stimulus duration

We first searched the whole brain for regions whose activation increased linearly with stimulus duration, separately within each modality. As shown in Figure 2 (first row), this contrast identified bilateral regions centered on the sensory cortices: the bilateral Heschl's gyri and neighboring sectors of the superior temporal gyrus for the auditory modality and two bilateral clusters extending from the occipital pole to lateral ventral temporal areas for the visual modality. In these regions, the responses were strictly unimodal, as attested by significant interactions between modality and duration (Table 1, Fig. 2). Plots of the hemodynamic responses in Heschl's gyrus and in left occipital cortex are presented in Figure 3. These plots clearly show that the amplitude and duration of the BOLD response were proportional to stimulus duration.

Regions with a collapse at the shortest duration of presentation

The above linear profile of BOLD variation with sentence duration was observed only in early sensory regions. In higher-order language areas, indeed, previous publications (Davis and Johnsrude, 2003; Friederici et al., 2010; Okada et al., 2010) led us to expect the fMRI signal to reflect the intelligibility associated with each compression condition rather than the physical compression rate itself. Indeed, many regions showed a nonlinear profile of activation with duration (Fig. 2, second row), showing virtually no variation as the sentences were compressed from 100% down to 40% (generally intelligible), and then a sudden collapse for the 20% condition (unintelligible). To identify all regions showing such a nonlinear collapse profile, we searched for voxels simultaneously passing a contrast indicating a nonlinear, steplike

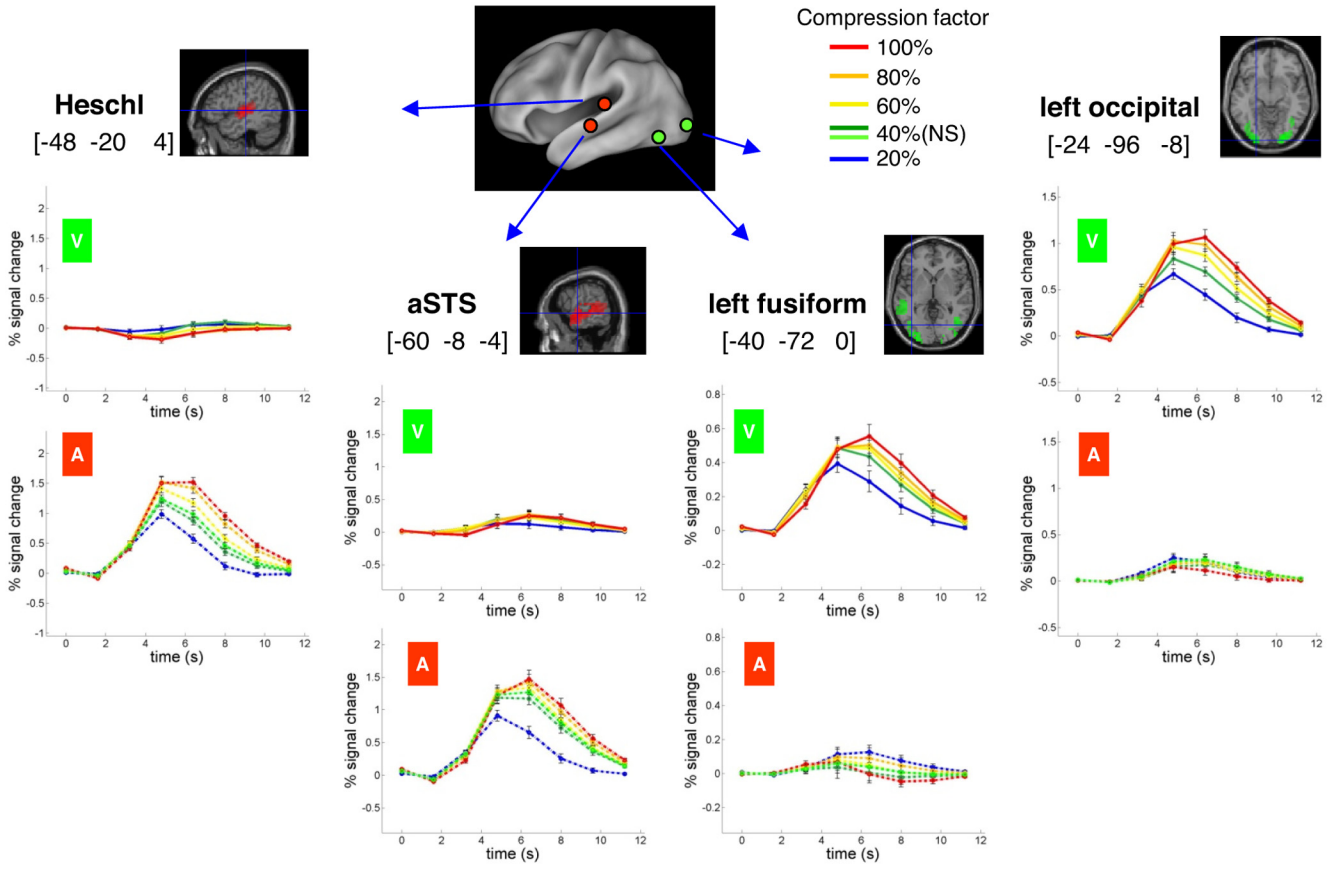

Figure 3. Time course of fMRI responses in modality-specific areas showing an increase of activation as a function of stimulus duration. Each ROI was defined as a sphere of 10 mm radius centered on the peak of the main effect reported in Table 1. Each panel shows the responses to written sentences (top, green V) and to spoken sentences (top, red A). Curve color indicates compression rate, with the warmest colors representing the slowest rates of sentence presentation (up to 100% compression factor = natural speech rate) and the coldest colors the fastest rates (down to 20% of original stimuli). For the auditory modality, the data are plotted separately for the two conditions at 40% compression factor (dark green, 40%N; light green, 40%S; see Materials and Methods). Sensory areas in occipital and Heschl's gyrus present a purely linear effect of duration. Left fusiform and aSTS regions, although presenting a superficially similar time course, exhibit a significant nonlinear component (interaction of modality with the nonlinear contrast [−4 1 1 1 1] exclusively masked by [0 3 1 −1 −3] and [0 −3 −1 1 3]; see Table 2).

profile of activation with duration and showing no significant linear variation in the range 40–100% (see Materials and Methods). Importantly, in most brain regions, these stringent conditions were frequently met simultaneously in both the auditory and the visual modalities (Fig. 2, blue regions). The amodal regions showing such a collapse effect included a large and bilateral extent of the superior temporal gyrus, extending toward the superior temporal sulcus and the middle temporal gyrus, and a left-hemispheric set of frontal regions including the inferior frontal gyrus and the precentral gyrus. The temporal response profile of these regions is plotted at the bottom of Figure 4. A nonlinear response can be seen most clearly in the posterior superior temporal sulcus (pSTS); the entire profile of the BOLD response remains identical as the sentence presentation is accelerated by a factor of 2.5 (from 100 to 40%). Such an invariant profile is remarkable given that, in sensory areas, we could easily identify changes in activation across these compression rates (Fig. 3).

Although the activation patterns for the nonlinear collapse contrast mostly overlapped across the auditory and visual modalities (Table 1), the interaction of this contrast with modality isolated two significant clusters described in Table 2. First, a nonlinear collapse unique to the visual modality was seen in the occipito-temporal cortex bilaterally, peaking in the left hemisphere at [−40 −72 0], and extending anteriorly to include the classical coordinates of the visual word form area (VWFA) ([−44 −54 −12]) (Cohen et al., 2000; Jobard et al., 2003; Cohen and Dehaene, 2004). Second, conversely, a nonlinear collapse unique to the auditory modality was found bilaterally within the superior temporal gyrus anterior to Heschl's gyrus, as well as the anterior STS (aSTS), including the coordinates of a putative homolog of the VWFA for the auditory modality [−60 −8 −4] (Cohen et al., 2004), an auditory region normalizing across voices and thus invariant to the surface form of speech stimuli (Dehaene-Lambertz et al., 2006). The time course of the BOLD response for these regions, shown in Figure 3 (center plots), appears as intermediate between that of purely sensory and purely collapsing regions; there is a small but nonsignificant difference between the compression factors 40–100% and a sudden though moderate drop of activation for the 20% condition.

Regions with maximal activation at intermediate durations

The third response profile that we searched for corresponded to regions with a peak activation at intermediate levels of compression. Such a profile might reflect the greater effort associated with understanding of moderately compressed sentences, as reflected behaviorally in slower response times to the intermediate levels of the compression factor (Fig. 1). The corresponding inverse quadratic contrast (see Materials and Methods), when pooling across the visual and auditory modalities, identified the anterior insula bilaterally, the bilateral supplemental motor area (SMA), extend-

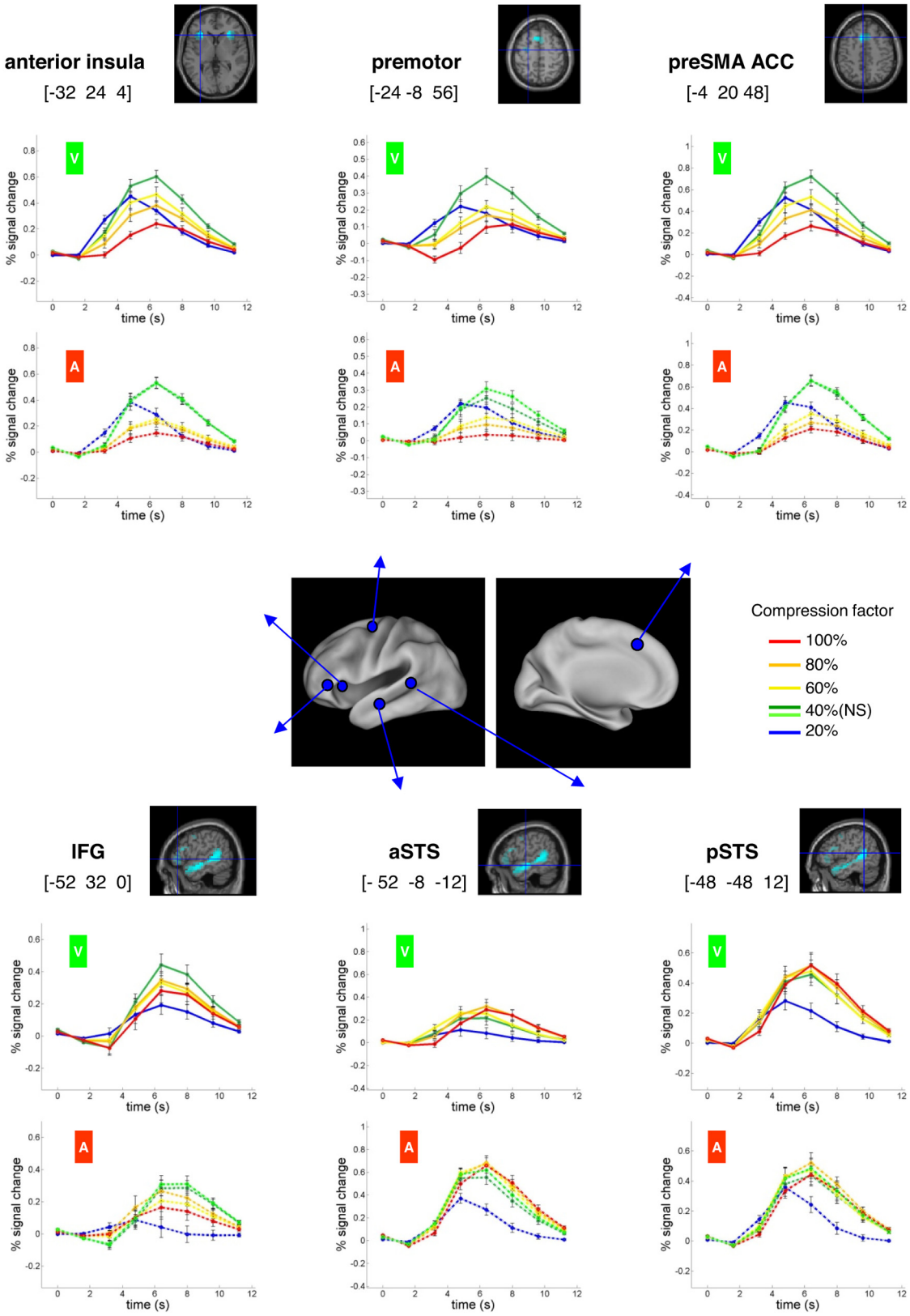

Figure 4. Time course of fMRI responses in regions exhibiting a nonlinear profile of activation as function of stimulus duration. Top, Regions showing a maximum of activation for intermediate compression factors (contrast [−2 1 2 1 −2] inclusively masked by [0 3 1 −1 −3]). Bottom, Regions exhibiting a collapse of activation at the fastest compression rate (20%) and a constant activation across all other compression factors (contrast [−4 1 1 1 1] exclusively masked with the two following contrasts [0 3 1 −1 −3] and [0 −3 −1 1 3]). Note that all these regions showed amodal profiles of activations similar in auditory (red A) and visual (green V) modalities.

Table 2. Coordinates of the significant activation peaks for the interactions of modality with each of the three contrasts described in Table 1

	A-V (mask A)					V-A (mask V)				
	MNI coordinates					MNI coordinates				
Brain area	*x*	*y*	*z*	Cluster size	*z* Score	*x*	*y*	*Z*	Cluster size	*z* Score
(A) Linear with duration										
L Heschl's gyrus	−44	−20	4	267	>8*	—	—	—	—	—
R Heschl's gyrus	52	−16	8	400	>8*	—	—	—	—	—
R inferior occipital gyrus	—	—	—	—	—	24	−92	−8	119	7.38*
L inferior occipital gyrus	—	—	—	—	—	−24	−96	−12	99	6.68*
L occipito-temporal sulcus	—	—	—	—	—	−40	−68	−8	99	3.86*
R occipito-temporal sulcus	—	—	—	—	—	48	−68	−4	28	4.47*
(B) Collapse for shortest										
L aSTS	−60	−8	−4	87	4.95*	—	—	—	—	—
L Insula	−40	−16	12	87	4.65*	—	—	—	—	—
R mSTS	52	−24	−4	33	4.66	—	—	—	—	—
R aSTS	60	8	−8	21	4.24	—	—	—	—	—
L mid occipital gyrus	—	—	—	—	—	−40	−72	0	71	3.98*
L inferior occipital gyrus	—	—	—	—	—	−32	−80	−8	71	3.65*
R inferior occipital gyrus	—	—	—	—	—	32	−80	−8	19	3.66
(C) Maximum for intermediate	—	—	—	—	—	—	—	—	—	—

To restrict analysis to active areas, interactions were masked inclusively by the corresponding contrast within the appropriate active modality [e.g., the A-V interaction was masked by (A)]. Same statistical thresholds as in Table 1.

ing into the anterior cingulate cortex (ACC), and a region of left premotor cortex. There was also a very small cluster (seven voxels) in the left inferior frontal gyrus (Fig. 2, third row). None of these regions were detected when an interaction with modality was computed, suggesting that this network is largely amodal. This conclusion was confirmed by analyses restricted to each modality (Table 1); most peaks were identified by the same inverse quadratic contrast within each modality, with the exceptions of the left premotor cortex, which attained significance only in the visual modality, and the left inferior frontal gyrus, in which the small cluster (six voxels) was observed only in the auditory modality.

The time course of the fMRI responses in representative ROIs is shown at the top of Figure 4. The largest responses were observed for the 40% compression condition, in both visual and auditory modalities (green curves). Above this compression rate (60–100%), the amplitude of the BOLD response decreased progressively (note that this pattern is opposite that observed in sensory areas) (Fig. 3). The response also became increasingly slower and flatter. Conversely, at the fastest compression factor (20%), which was not intelligible, only an early, brief, yet quite intense BOLD response was observed.

Regions whose activation decreased with increasing stimulus duration

A fourth response profile, i.e., a linear decrease as stimulus duration increased, accounted for the remaining brain regions (those achieving significance in an overall *F* test for presentation rate; see Materials and Methods). This linearly decreasing contrast was significant across both auditory and visual modalities in a broad set of regions (Fig. 2, bottom row). Highly significant decreases were seen in the bilateral anterior prefrontal regions ([−28 48 12], [28 56 12]) and midline anterior cingulate ([−4 28 36]), where activation was primarily seen during the 20% and 40% compression factors and became nonsignificant for slower presentation rates. These activations might therefore correspond to a brain network for sustained effort related to the greater difficulty and task engagement needed at high sentence presentation rates. A similar pattern, though with a more continuous decrease in activation with stimulus duration, was seen in the SMA [−4 −8 52], bilateral inferior parietal cortex ([−40 −48 44], [48 −44 48]), and insula ([−40 0 8], [40 4 8]). Finally, a special case was the left motor/post-central cortex, whether the temporal profile of activation disclosed an increasingly delayed response with longer stimulus duration, as would be expected from the fact that subjects responded with their right hand at the end of each sentence.

All the above regions reached significance in both the auditory and the visual modalities. In addition, we observed a significant interaction with modality, indicating a decreasing BOLD effect restricted to the visual modality, in bilateral mesial occipital (cuneus) ([−12 −76 32], [16 −68 28]), bilateral lingual gyrus ([−8 −80 −4], [8 −80 0]), and bilateral Heschl's gyrus, with a stronger effect on the left [−44 −12 8] than on the right [44 −8 8]. Plots (Fig. 3, see examples) showed that all these sites exhibited a deactivation evoked by the visual sentence, whose depth and duration were proportional to sentence duration. These findings may therefore correspond to an active inhibition of regions not needed for the foveal reading task, both in primary auditory cortex and in visual cortex responsive to the periphery of the visual field (Corbetta and Shulman, 2002; Hasson et al., 2002). In the converse direction, no region showed a greater decrease in activation in the auditory modality compared with the visual modality.

Activations linked to intelligibility

At the 40% compression rate, self-reported intelligibility was highly variable from trial to trial. To explore the cerebral correlates of intelligibility, we searched for areas in which the BOLD signal was linearly correlated with intelligibility ratings within the 40% conditions (pooling across both modalities; see Materials and Methods). At the FDR corrected-level threshold of $p < 0.05$, no significant activation was detected. However, at an uncorrected voxel-based threshold of $p < 0.001$ (and cluster size >10 voxels), a set of areas restricted to the left hemisphere was found, overlapping with the classical perisylvian areas known to be involved in sentence comprehension (Fig. 5): aSTS ([−48 −8 −16], $z = 4.12$, 37 voxels), pSTS ([−48 −40 0], $z = 3.85$, 53 voxels), temporal pole ([−44 8 −32], $z = 3.45$, 13 voxels). Another cluster of 29 voxels was found in the parietal lobe, including the supramarginal gyrus and the angular gyrus ([−60 −60 24], $z = 3.71$ and [−48 −48 28], $z = 3.66$). Finally, two clusters were

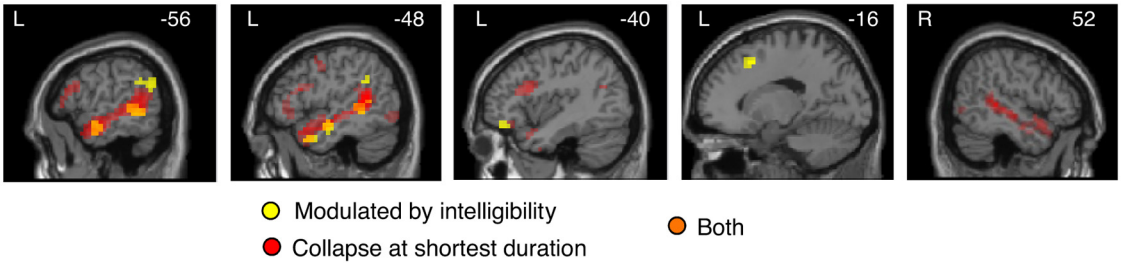

Figure 5. Regions modulated by subjective intelligibility. Yellow, Regions in which activation amplitude was significantly correlated with subjective ratings of intelligibility for sentences presented at 40% compression rate (where intelligibility varied the most across trials). In the STS, most of these regions overlapped with regions showing a nonlinear activation across compression factors (red voxel). The intersection of the two contrasts appears in orange.

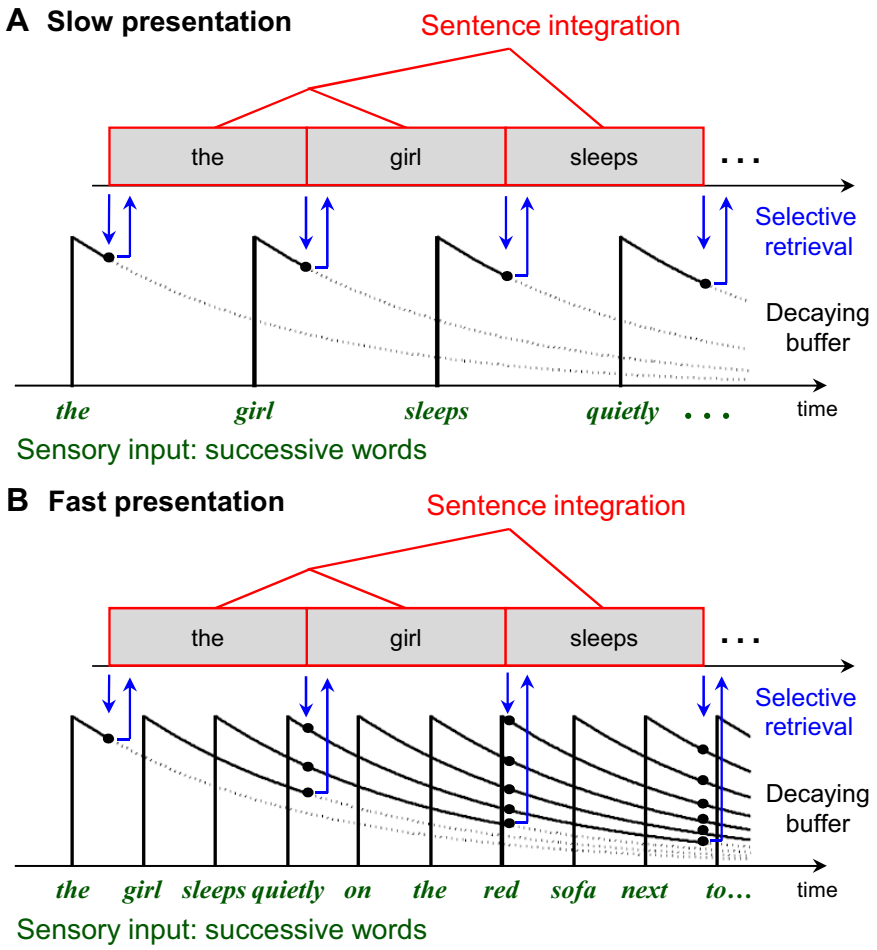

Figure 6. Schematic model of a temporal bottleneck during sentence integration. The model assumes that the integration of successive words into a unified syntactic and semantic structure proceeds at a relatively fixed pace (gray boxes within each panel). Incoming words have to be temporarily stored in a buffer, here assumed to decay exponentially, before being transmitted to the sentence integration stage. ***A***, When words are presented at a slow rate, buffer storage and retrieval proceeds without any difficulty as only one word, or just a few, is waiting at any given moment. ***B***, When words are presented at a fast rate, however, they pile up in the buffer, thus complicating their retrieval. Note that the least recent word must be selectively retrieved ("first in, first out" principle). We assume that buffer retrieval collapses totally once the number of buffered words exceeds a certain value.

observed in the frontal lobe, in the pars orbitalis ($[-44\ 40\ -16]$, $z = 3.68$, 14 voxels), and in the superior medial frontal cortex ($[-16\ 16\ 48]$, $z = 4.08$, 17 voxels). There was no activation in the right hemisphere, even at a more lenient threshold of $p < 0.01$ voxel based.

As shown in Figure 5, most of the above areas modulated by intelligibility overlapped with those showing a collapse at the shortest duration of sentence presentation. Thus, these two independent criteria converge to suggest that activation in left superior temporal and inferior frontal regions drops to a near-zero level when sentences cease to be intelligible, in agreement with previous findings (Davis and Johnsrude, 2003; Friederici et al., 2010; Okada et al., 2010). An exception was the temporal parietal junction, which was modulated by intelligibility but did not show a collapse at short sentence duration. Instead, this region showed an overall deactivation during sentence processing, which tended to be larger for longer sentence duration.

Proposed model

Our finding of an invariant brain activation in major high-level perisylvian language regions (Fig. 4, bottom), in spite of a near doubling of sentence presentation speed (from 100 to 60% of original duration) is a salient observation that suggests that the cortical processing speed of sentences is tightly constrained and cannot be easily accelerated. We now flesh out a detailed theoretical interpretation based on this insight. We show that the simple hypothesis of a temporal bottleneck can account for the existence of three distinct types of brain regions, each with a distinct temporal profile of activation as a function of compression rate and input modality, and leads to verifiable predictions concerning the phase of their BOLD response.

The main premise of our model is that the higher-level processes of language comprehension, where words are integrated into syntactic and semantic constituents, are relatively slow, cannot easily accelerate their processing speed, and therefore impose a processing bottleneck. When words are presented at a slow enough pace, equal to or slower than this internal processing speed, each word can be processed immediately and language comprehension proceeds at a speed limited only by the sensory stream. However, when words are presented at a faster speed, exceeding the internal processing speed, some words cannot be processed immediately. Our model assumes that they have to be temporarily stored in a buffer from

which they will be later retrieved once the central language comprehension system becomes available. At this point, sentence comprehension speed becomes solely determined by the internal processing speed and ceases to accelerate with the pace of the incoming sensory stimuli. This phenomenon is analogous to the well studied psychological refractory period (PRP) phenomenon in dual-task processing; in a broad variety of cognitive tasks, when two successive targets, T1 and T2, are presented in close temporal succession, the processing of the second target, T2, has to wait in a buffer until completion of the processing of target T1, resulting in a demonstrable slowing down of the response time to T2 (Pashler, 1994; Sigman and Dehaene, 2008; Zylberberg et al., 2010). Similarly, here, we argue that when many words are presented in close temporal proximity, the most recent ones may have to wait in a buffer before being integrated at the sentence level.

A major difference between the present task and the classic PRP phenomenon is that not just two targets, but a total of 12 words, are successively presented. Thus, participants must be able to hold several words in the buffer and to selectively retrieve them in the appropriate order. Our hypothesis is that buffering and selective retrieval pose increasing difficulties as the number of buffered words increases. Figure 6 illustrates one possible mechanism that could underlie this increase in difficulty. As in a recent neuronal model of the PRP (Zylberberg et al., 2010), our diagram assumes that, in the buffer, the internal representation of words decays exponentially with time. As more and more words are presented at a fast pace, the selection of which word to transmit to sentence integration processes becomes increasingly difficult, both because more and more words are present in the buffer but also because it is the oldest and therefore the least active word that has to be retrieved. The model predicts that sentence processing will ultimately collapse once the input stream becomes so fast as to necessitate an exceedingly large number of words to be stored and retrieved from the buffer. This collapse may be functionally analogous to the "attentional blink," i.e., the finding that, during the processing of a first target, a second target may be missed and remain subjectively undetected (Raymond et al., 1992; Sergent and Dehaene, 2004).

Just as the complexity and processing time of the first target modulates the attentional blink (Jolicoeur, 1999), our model predicts that, during the comprehension of compressed sentences, the difficulty of the preceding word integration operations should modulate the critical temporal pace at which comprehension collapses. While we used simple right-branching sentences, which remain understandable at a fast rate, the model predicts that more complex sentences, for instance those including object relatives or passives, would impose a slower internal processing time and therefore would require a slower presentation mode (Just et al., 1996b; Stromswold et al., 1996). These temporal difficulties would be compounded in aphasic patients, in whom

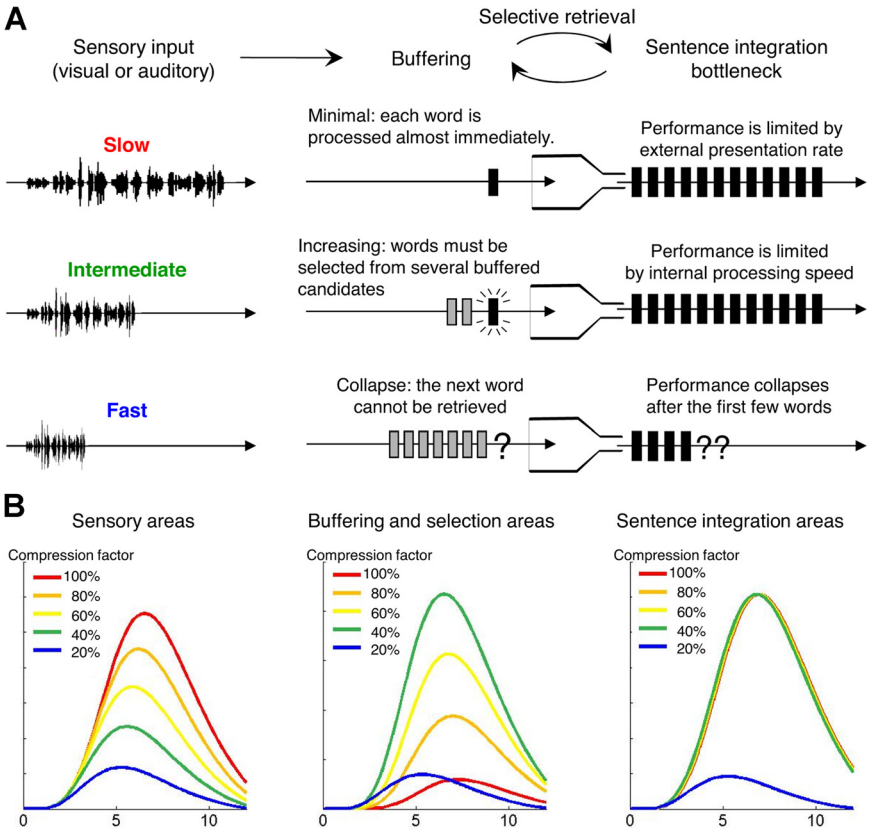

Figure 7. fMRI activation patterns predicted by the bottleneck model. ***A***, Schematic depiction of the amount of processing required by a 12-word sentence presented at three different paces (rows: slow, intermediate, fast) at each of the three different stages of the proposed model (columns: sensory, buffer, integration). ***B***, Predicted time course of fMRI responses predicted by computer simulations at each of these stages, as the compression factor is varied from 20 to 100%. The simulated curves can be directly compared with the experimental data in Figures 3 and 4.

delayed grammatical responses have indeed been observed using the fine temporal resolution of event-related potentials (Swaab et al., 1998; ter Keurs et al., 1999, 2002; Wassenaar and Hagoort, 2005). Finally, although Figure 6, for simplicity, depicts a feedforward model, psycholinguistic research suggests that top-down predictive operations play an essential role in facilitating the integration of novel incoming words (Konieczny, 2000; Altmann and Mirkovic, 2009). Our model therefore predicts that words and structures that are predictable given past inputs should encumber the buffer for a shorter duration, leading to a lower compression threshold when the words are predictable than when they are not.

In all these respects, our model bears some similarity to Just and Carpenter's Capacity Theory of Sentence Comprehension (Just and Carpenter, 1992; MacDonald et al., 1992; Just et al., 1996a). This theory postulates that a working memory buffer plays an essential role in maintaining active representations of words during syntactic comprehension and that saturation of its capacity (which may vary across individuals) may cause comprehension difficulties. Two important differences, however, are that (1) our proposal is not committed to the hypothesis that syntactic comprehension relies on the same working memory buffer as other explicit verbal tasks (Waters and Caplan, 1996) [rather, the buffer may be implemented by local, dedicated, and passively decaying reverberating circuits (Zylberberg et al., 2009)] and (2) while Just and Carpenter (1992) give working memory a decisive role in a variety of linguistic manipulations (e.g., comprehension of passive sentences, maintenance of mul-

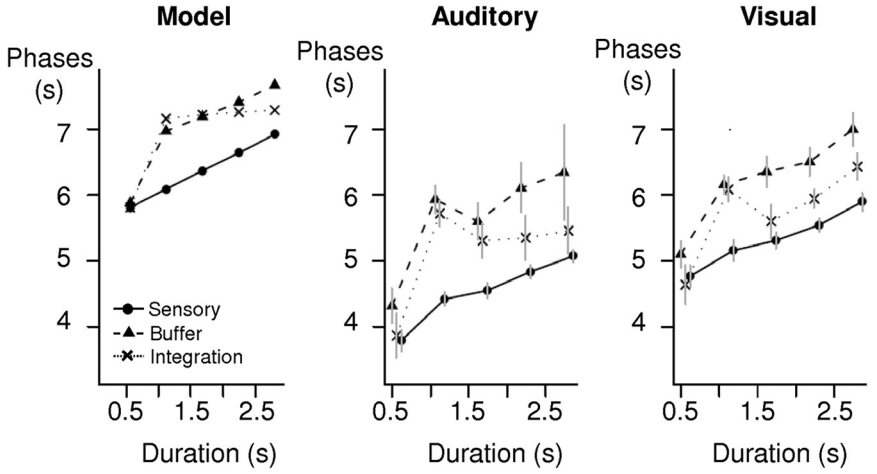

Figure 8. Predicted and observed phases of the fMRI activation as a function of sentence duration. Left, Quantitative theoretical predictions for the three types of regions postulated in the model (sensory, buffer, integration). The phases in seconds were estimated by fitting a sinusoidal function of the time courses presented in Figure 7. Middle and right, Observed fMRI phases in the left hemisphere, separately for the auditory and visual modalities. All ROIs located in the left hemisphere and reported in Table 1 were averaged together, separately for the three types of regions defined by the SPM contrasts in Figure 1 and Table 1.

tiple ambiguous meanings), we merely propose an input buffer whose sole role is to maintain incoming words until they are integrated at the sentence level. We performed computer simulations of our model, using the following minimal assumption: internal processing time = 250 ms/word, buffer limit = 7 words (the qualitative predictions are independent of these choices). As shown in Figure 7, once convolved with the standard hemodynamic response function, our model reproduces many of the details of the observed fMRI activation profiles. Three types of brain regions are predicted. Sensory regions should show monotonically increasing and delayed activations as a function of increasing stimulus duration. Activity in buffer/selection regions should follow an inverted U curve with maximal activity for intermediate durations. Finally, regions involved in sentential integration should show invariant activations up to a certain compression factor and a sudden collapse when buffer or selection capacity is exceeded. Obviously, the three predicted profiles are similar to those identified in our empirical fMRI measurements.

Phase analysis of fMRI activation

The model makes further predictions concerning the timing of fMRI activations (Figs. 7, 8). For sensory regions before the postulated bottleneck, because activation duration is strictly proportional to stimulation duration, the phase of the fMRI response should increase linearly with sentence duration. Furthermore, the slope of that increase, measuring the amount of fMRI activation delay for each second of additional stimulation, should be 0.50, as any change in the duration of neural activation translates into a shift of the peak fMRI response by half this value (Sigman et al., 2007). For buffer/selection regions, our simulations predict a nonlinear profile with fast responses in the 20% condition (buffer saturated and nonoperative), and suddenly slower BOLD responses at slower rates, with an increase of phase delay at slower presentation rates (predicted slope = 0.40). Finally, for post-bottleneck sentential integration, we also predict a nonlinear profile but, as seen in Figures 7 and 8, now with a constant phase delay (slope = 0) for all intelligible conditions (>40% compression rate). Note that this prediction is parameter dependent; it assumes that, for our stimuli, processing time is determined by the internal processing speed rather than the external stimulation rate. A small increase would be predicted if, at the slowest rate, sentences began to be presented more slowly than the internal integration rate.

One last counterintuitive prediction is noteworthy. The model predicts that buffer/selection regions, although involved in an intermediate processing stage (between sensory processing and sentence integration), should show the slowest absolute fMRI phase, slower than sentential integration. The reason is that, while sentence integration proceeds continuously throughout the presentation of the successive words, the buffer is not needed for processing the first incoming words, especially at slow presentation rates, and is maximally involved only toward the end of the sentence.

To test these predictions, we extracted the phase of the BOLD response within ROIs defined as 10 mm spheres centered on peaks identified by the standard SPM analysis (Table 1), separately for each compression factor (20, 40, 60, 80, 100%), each modality, and each subject. We restricted our analysis to the left hemisphere because phase estimates were insufficiently stable for the right hemisphere, where activation was smaller. Because phase extraction from single-subject data is inherently noisy, the phases were averaged together (using the circular mean) for ROIs obtained through a given contrast (i.e., linear with duration, maximum for intermediate duration, and collapse for shortest duration), resulting in one phase measure per participant for each experimental condition and each of the three region types. This allowed us to directly compare them to the predictions of the regions introduced in the model respectively as sensory, buffer/selection, and sentence integration regions.

Figure 8 shows the mean phase in these three types of regions, as a function of stimulus duration and modality. The profiles were similar for auditory and visual stimulation and globally resembled those predicted by the model (leaving aside an overall shift probably due to an imperfect onset-delay parameter of the standard hemodynamic function in SPM, used to generate the theoretical predictions). We first tested the prediction that the impact of sentence duration on the phase of the activation should differ across the three region types. Thus, we computed an ANOVA with region type (three levels) and compression factor as within-subject variables, separately for each modality (because the sensory ROIs differed in each modality). In each modality, the main effects of region type and of compression rate were significant ($p < 10^{-3}$). Crucially, the interaction between the two factors was significant in the visual modality [$F_{(8,120)} = 2.68$, $p < 0.01$] and approached significance in the auditory modality [$F_{(8,120)} = 1.92$, $p < 0.06$].

For sensory regions, we observed exactly the predicted linear increase in phase with stimulus duration. We used a linear regression to estimate the slope with which the phase in sensory regions increased as a function of sentence duration (Sigman et al., 2007). For both visual and auditory modalities, the observed slopes were both significantly different from zero ($p < 0.001$) and did not differ significantly from the value of 0.50 predicted under the hypothesis that the duration of neural activity is directly related to stimulus duration (auditory slope = 0.54; visual slope = 0.47).

The model also predicted that buffer and sentence integration regions should show a slower overall phase than sensory regions,

at all but the shortest sentence duration (Fig. 7, left). Therefore, we used ANOVAs to compare the phases in sensory regions with those in buffer regions and, separately, in sentence integration regions. When comparing buffer and sensory regions, in both modalities, the phase was shorter overall in sensory regions (auditory: $F_{(1,15)} = 46.9, p < 10^{-3}$; visual: $F_{(1,15)} = 24.1, p < 10^{-3}$). The predicted region by duration interaction was only significant in the visual modality ($F_{(4,60)} = 3.83, p < 0.01$), not the auditory modality ($F_{(4,60)} = 1.28, p < 0.30$). When comparing sensory and sentence integration regions, the phase was shorter in sensory regions in both modalities (auditory: $F_{(1,15)} = 6.21, p < 0.05$; visual: $F_{(1,15)} = 7.56, p < 0.05$), with a significant region by duration interaction (auditory: $F_{(4,60)} = 19.8, p < 10^{-3}$; visual: $F_{(4,60)} = 4.12, p < 10^{-2}$).

The model predicted a subtle difference in the phase of buffer versus sentence integrations; in the intelligible range (40–100% compression factors), the phase should stay constant for sentence integration regions (predicted slope = 0) but should increase for buffer regions (predicted slope = 0.40). Indeed, for the buffer regions, the regression slopes restricted to the range 40–100% were 0.38 and 0.53, respectively, for auditory and visual modality. These values were significantly higher than zero ($p < 0.001$) and not significantly different from the value of 0.40 expected from the model. Furthermore, slopes were significantly higher for buffer regions than for sentence integration regions ($p < 0.001$), and the differences in slopes (0.58 and 0.28, respectively) did not differ significantly from the predicted value of 0.40. For sentence integration regions, the slope was close to the predicted value of zero in the auditory modality (slope = −0.21, not significant). However, it was significantly positive, with a mean of 0.26, in the visual modality ($p < 0.001$), the only significant deviation from the model. Examination of the fMRI response confirmed a small acceleration with presentation speed in the visual modality, an effect that was not seen with auditory sentences (Fig. 4, region pSTS). This observation suggests that the internal processing speed may be slightly faster for visual sentences than for auditory sentences, so that the visual sentences presented at 100% rate (257 wpm) were below the maximal processing speed.

Finally, we used ANOVAs to compare the absolute phases in buffer regions with sentence integration regions. As predicted, the absolute phase of the fMRI activation was shorter in sentence integration than in buffer regions for written sentences (visual: $F_{(1,15)} = 4.63, p < 10^{-2}$) and marginally so for spoken sentences ($F_{(1,15)} = 3.85, p < 0.07$).

Discussion

We parsed brain areas according to their fMRI response to five levels of sentence compression, ranging from intelligible (100–60%) to challenging (40%) and to incomprehensible (20%). Early sensory regions showed a linear acceleration paralleling stimulus duration. However, perisylvian language areas in the left STS and inferior frontal gyrus demonstrated a temporally invariant response profile up to ~40% compression, followed by a sudden collapse. These results confirm an association of language intelligibility with the left perisylvian inferior frontal gyrus and the superior temporal gyrus (Davis and Johnsrude, 2003; Davis et al., 2007), including for compressed speech (Poldrack et al., 2001; Peelle et al., 2004, 2010; Adank and Devlin, 2010). Adank et al. (2010) found that, as subjects adapt to compressed speech, activation increases in bilateral superior temporal and midline premotor cortices. Our results complement this study by showing that, even for a fixed presentation duration, spontaneous fluctuations in intelligibility are also associated with the same network (Fig. 5).

By varying word rate, several studies observed that activation amplitude in regions surrounding the primary sensory cortices varies linearly with stimulus duration (Binder et al., 1994; Dhankhar et al., 1997; Buchel et al., 1998; Poldrack et al., 2001), while other regions show a quadratic variation (Binder et al., 1994; Buchel et al., 1998; Poldrack et al., 2001) or a peak of activation at the fastest presentation rate (Peelle et al., 2004). However, previous studies used block designs, which prevents identification of the temporal response profile and drastically complicates modeling and interpretation. For instance, Poldrack et al. (2001) used a fixed interstimulus interval within each block, thus introducing a confound (at faster compression rates, more sentences are presented). Furthermore, Adank et al. (2010) modeled the fMRI activation using predictors whose durations were proportional to the presentation duration, thus implicitly assuming a linear variation of neural activity.

Event-related fMRI allowed us to bypass these problems and observe both the amplitude and the delay of fMRI activation evoked by a single compressed sentence. Our findings confirm that fMRI can have a high temporal resolution (Menon et al., 1998; Sigman et al., 2007; Sigman and Dehaene, 2008). Sensory areas showed the fastest BOLD response to language, followed by left superior temporal sulcus and inferior frontal regions, replicating earlier observations (Dehaene-Lambertz et al., 2006; Brauer et al., 2008; Pallier et al., 2011). Importantly, these delays cannot be solely due to inflexible hemodynamics, as they vary with sentence repetition (Dehaene-Lambertz et al., 2006), syntactic complexity (Pallier et al., 2011), and word rate (present study). They are also too large to arise merely from synaptic propagation of the language input into the temporal and frontal lobes. Tentatively, they might reflect information integration operating over increasingly larger speech units, from individual phonemes to words, phrases, or prosodic patterns, therefore requiring longer integration time and more sustained activity (Dehaene-Lambertz et al., 2008).

Although the compression rates of 60, 80, and 100% were all associated with near-perfect sentence intelligibility and thus constant behavior, they modulated brain activation profiles. In sensory regions, both activation amplitude and peak delay were reduced by language compression, as expected from a simple convolution of the hemodynamic response function with a neural activation proportional to stimulus duration. However, other regions attributed to the postulated buffer (e.g., inferior frontal gyrus/anterior insula) exhibited a nontrivial profile consisting in an accelerated activation but with an increasing amplitude as sentence duration decreased, for both written and spoken sentences. Finally, left inferior frontal gyrus and STS showed a constant activation profile, both in time and in amplitude, over the intelligible compression range, followed by a collapse at unintelligible rates (a profile again independent of input modality).

Our results indicate that the majority of left-hemispheric areas classically associated with higher-level language processing (Saur et al., 2010; Pallier et al., 2011) exhibit, for both written and spoken language, temporally stable responses that cannot be accelerated much beyond the rate that served as our 100% baseline (256 wpm). These findings are strongly suggestive of a temporal bottleneck. We therefore propose that the classical bottleneck model of dual-task processing should be extended to the specific multitasking problem posed by fast language comprehension. In dual tasks, participants process two successive targets at a very short interval. Behavior and brain imaging results indicate that,

while perceptual processing remains on-line with the stimuli, a "central" decision associated with distributed parietal and prefrontal areas is delayed for the second stimulus (Pashler, 1984; Raymond et al., 1992; Marois and Ivanoff, 2005; Dux et al., 2006; Sigman and Dehaene, 2008). Similarly, here, by imposing a fast rate of stimulus presentation (with 12 successive words instead of just two targets), we find that higher-level language areas cannot keep up with stimulus rate. As in the dual-task paradigm, incoming stimuli are not processed immediately but, rather, after a delay. Thus, a buffer system is required to temporarily store the incoming words and retrieve them when higher-level processing has become available. As the stimulus rate increases, more and more words have to be stored in the buffer. This model predicts a joint acceleration and increase of the BOLD response in buffer and selective retrieval areas, precisely as observed in the left inferior frontal/anterior insula, precentral cortex, and mesial frontal cortex.

Note that in the dual-task paradigm, the buffer is typically modeled as a passive system in which information decays (Zylberberg et al., 2009) and which, therefore, does not impose additional activation but merely a pure delay (Jiang et al., 2004). Here, however, multiple words must be stored and retrieved in the correct temporal order. This need for selective retrieval may explain the increasing prefrontal and precentral activations as presentation rate increased. Interestingly, the observed buffer/selection areas include a left precentral region plausibly overlapping with the left frontal eye field (FEF; coordinates [−24 −8 56]). During self-paced reading, retrieval of the next word requires reorienting the eyes, which involves the FEF. It is interesting that the same region is also involved when retrieving the next word from an internal memory buffer during RSVP.

Most important, our results clarify the mechanisms underlying the sudden collapse of language comprehension when word rate exceeds a certain threshold. We suggest that the main factor is not a sensory limitation but a central amodal processing bottleneck that leads to the overflow of an internal buffer. For simplicity, our model assumed that beyond a fixed number of stored words, buffer retrieval collapses. However, several additional factors may conspire to produce a nonlinear collapse of intelligibility at fast presentation rates, e.g., exponential memory decay (Sperling, 1960; Lu et al., 2005; Zylberberg et al., 2009), number of competing words, and visual, phonological, syntactic, or semantic confusability.

At the fastest presentation rate of 20%, where words were presented every 46 ms on average, stimulus degradation and masking of each word by the next are also likely factors (Del Cul et al., 2007). A masking effect could explain the reduced activation in left ventral occipito-temporal cortex, near the site of the VWFA, specifically at 20% compression rate. Nevertheless, sensory limitations alone cannot explain the important drop in intelligibility already observed at 40% compression (93 ms/word) for both spoken and written sentences. Visually, 93 ms/word is outside the masking range (Del Cul et al., 2007) and well within the temporal tracking capacity of visual cortex (Forget et al., 2009) and VWFA (Dehaene et al., 2001). Auditorily, intracranial recordings have documented "the ability of the core auditory cortex to follow the temporal speech envelope over a wide range of speaking rates" (Nourski et al., 2009) (see also Giraud et al., 2000). Indeed, fMRI signals from sensory areas faithfully tracked the duration of incoming visual or auditory stimuli (see also Binder et al., 1994; Dhankhar et al., 1997; Buchel et al., 1998). Furthermore, the pSTS showed a constant activation even for 40% compressed stimuli, suggesting that, at this presentation rate at least, the stimuli still underwent high-level processing and were limited by a later, postsensory stage.

As a final argument against a dominant role of sensory limitations, Ghitza and Greenberg (2009) showed that, starting with incomprehensible sentences compressed at 33%, intelligibility could be recovered by inserting silent intervals. This finding shows that enough sensory information was still present in the compressed signal and fits with our bottleneck hypothesis; for equal signal quality, the insertion of silence provides additional processing time and therefore prevents buffer saturation.

The fast compression threshold that we observed may be due to our use of simple right-branching sentence structures. Our model predicts that the threshold should vary with the complexity of sentence integration operations. For instance, significantly more time should be required for object than for subject relatives (Just et al., 1996b; Stromswold et al., 1996). At one extreme, asking subjects to process lists of unconnected words should lead to a collapse at a much slower rate than for sentences, as observed behaviorally (Potter et al., 1980). Time-resolved fMRI may help test these ideas, but it can only coarsely estimate the onset and duration of the overall activation evoked by a set of words. Future studies could use magneto- or electro-encephalography to provide a higher temporal resolution on the word-by-word pace of language comprehension.

References

Adank P, Devlin JT (2010) On-line plasticity in spoken sentence comprehension: adapting to time-compressed speech. Neuroimage 49:1124–1132.

Altmann GT, Mirković J (2009) Incrementality and prediction in human sentence processing. Cogn Sci 33:583–609.

Binder JR, Rao SM, Hammeke TA, Frost JA, Bandettini PA, Hyde JS (1994) Effects of stimulus rate on signal response during functional magnetic resonance imaging of auditory cortex. Brain Res Cogn Brain Res 2:31–38.

Brauer J, Neumann J, Friederici AD (2008) Temporal dynamics of perisylvian activation during language processing in children and adults. Neuroimage 41:1484–1492.

Brennan J, Nir Y, Hasson U, Malach R, Heeger DJ, Pylkkänen L (2012) Syntactic structure building in the anterior temporal lobe during natural story listening. Brain Lang 120:163–173.

Büchel C, Holmes AP, Rees G, Friston KJ (1998) Characterizing stimulus-response functions using nonlinear regressors in parametric fMRI experiments. Neuroimage 8:140–148.

Chodorow MS (1979) Time compressed speech and the study of lexical and syntactic processing. In: Sentence processing (Cooper WE, Walker ECT, eds), pp 87–111. Hillsdale, NJ: Erlbaum.

Cohen L, Dehaene S (2004) Specialization within the ventral stream: the case for the visual word form area. Neuroimage 22:466–476.

Cohen L, Dehaene S, Naccache L, Lehéricy S, Dehaene-Lambertz G, Hénaff MA, Michel F (2000) The visual word form area: spatial and temporal characterization of an initial stage of reading in normal subjects and posterior split-brain patients. Brain 123:291–307.

Cohen L, Jobert A, Le Bihan D, Dehaene S (2004) Distinct unimodal and multimodal regions for word processing in the left temporal cortex. Neuroimage 23:1256–1270.

Corbetta M, Shulman GL (2002) Control of goal-directed and stimulus-driven attention in the brain. Nat Rev Neurosci 3:201–215.

Davis MH, Johnsrude IS (2003) Hierarchical processing in spoken language comprehension. J Neurosci 23:3423–3431.

Davis MH, Coleman MR, Absalom AR, Rodd JM, Johnsrude IS, Matta BF, Owen AM, Menon DK (2007) Dissociating speech perception and comprehension at reduced levels of awareness. Proc Natl Acad Sci U S A 104:16032–16037.

Dehaene S, Naccache L, Cohen L, Bihan DL, Mangin JF, Poline JB, Rivière D (2001) Cerebral mechanisms of word masking and unconscious repetition priming. Nat Neurosci 4:752–758.

Dehaene-Lambertz G, Dehaene S, Anton JL, Campagne A, Ciuciu P, Dehaene GP, Denghien I, Jobert A, Lebihan D, Sigman M, Pallier C, Poline JB (2006) Functional segregation of cortical language areas by sentence repetition. Hum Brain Mapp 27:360–371.

Dehaene-Lambertz G, Hertz-Pannier L, Dubois J, Dehaene S (2008) How

does early brain organization promote language acquisition in humans? Eur Rev 16:399–411.
Del Cul A, Baillet S, Dehaene S (2007) Brain dynamics underlying the nonlinear threshold for access to consciousness. PLoS Biol 5:e260.
Dhankhar A, Wexler BE, Fulbright RK, Halwes T, Blamire AM, Shulman RG (1997) Functional magnetic resonance imaging assessment of the human brain auditory cortex response to increasing word presentation rates. J Neurophysiol 77:476–483.
Dupoux E, Green K (1997) Perceptual adjustment to highly compressed speech: effects of talker and rate changes. J Exp Psychol Hum Percept Perform 23:914–927.
Dux PE, Ivanoff J, Asplund CL, Marois R (2006) Isolation of a central bottleneck of information processing with time-resolved FMRI. Neuron 52:1109–1120.
Forget J, Buiatti M, Dehaene S (2010) Temporal integration in visual word recognition. J Cogn Neurosci 22:1054–1068.
Friederici AD, Kotz SA, Scott SK, Obleser J (2010) Disentangling syntax and intelligibility in auditory language comprehension. Hum Brain Mapp 31:448–457.
Ghitza O, Greenberg S (2009) On the possible role of brain rhythms in speech perception: intelligibility of time-compressed speech with periodic and aperiodic insertions of silence. Phonetica 66:113–126.
Giraud AL, Lorenzi C, Ashburner J, Wable J, Johnsrude I, Frackowiak R, Kleinschmidt A (2000) Representation of the temporal envelope of sounds in the human brain. J Neurophysiol 84:1588–1598.
Hasson U, Levy I, Behrmann M, Hendler T, Malach R (2002) Eccentricity bias as an organizing principle for human high-order object areas. Neuron 34:479–490.
Hasson U, Yang E, Vallines I, Heeger DJ, Rubin N (2008) A hierarchy of temporal receptive windows in human cortex. J Neurosci 28:2539–2550.
Jiang Y, Saxe R, Kanwisher N (2004) Functional magnetic resonance imaging provides new constraints on theories of the psychological refractory period. Psychol Sci 15:390–396.
Jobard G, Crivello F, Tzourio-Mazoyer N (2003) Evaluation of the dual route theory of reading: a meta-analysis of 35 neuroimaging studies. Neuroimage 20:693–712.
Jolicoeur P (1999) Concurrent response-selection demands modulate the attentional blink. J Exp Psychol Hum Percept Perform 25:1097–1113.
Just MA, Carpenter PA (1992) A capacity theory of comprehension: individual differences in working memory. Psychol Rev 99:122–149.
Just MA, Carpenter PA, Woolley JD (1982) Paradigms and processes in reading comprehension. J Exp Psychol Gen 111:228–238.
Just MA, Carpenter PA, Keller TA (1996a) The capacity theory of comprehension: new frontiers of evidence and arguments. Psychol Rev 103:773–780.
Just MA, Carpenter PA, Keller TA, Eddy WF, Thulborn KR (1996b) Brain activation modulated by sentence comprehension. Science 274:114–116.
Konieczny L (2000) Locality and parsing complexity. J Psycholinguist Res 29:627–645.
Lerner Y, Honey CJ, Silbert LJ, Hasson U (2011) Topographic mapping of a hierarchy of temporal receptive windows using a narrated story. J Neurosci 31:2906–2915.
Lu ZL, Neuse J, Madigan S, Dosher BA (2005) Fast decay of iconic memory in observers with mild cognitive impairments. Proc Natl Acad Sci U S A 102:1797–1802.
MacDonald MC, Just MA, Carpenter PA (1992) Working memory constraints on the processing of syntactic ambiguity. Cogn Psychol 24:56–98.
Marois R, Ivanoff J (2005) Capacity limits of information processing in the brain. Trends Cogn Sci 9:296–305.
Mehler J, Sebastian N, Altmann G, Dupoux E, Christophe A, Pallier C (1993) Understanding compressed sentences: the role of rhythm and meaning. Ann N Y Acad Sci 682:272–282.
Menon RS, Luknowsky DC, Gati JS (1998) Mental chronometry using latency-resolved functional MRI. Proc Natl Acad Sci U S A 95:10902–10907.
Nourski KV, Reale RA, Oya H, Kawasaki H, Kovach CK, Chen H, Howard MA 3rd, Brugge JF (2009) Temporal envelope of time-compressed speech represented in the human auditory cortex. J Neurosci 29:15564–15574.
Okada K, Rong F, Venezia J, Matchin W, Hsieh IH, Saberi K, Serences JT, Hickok G (2010) Hierarchical organization of human auditory cortex: evidence from acoustic invariance in the response to intelligible speech. Cereb Cortex 20:2486–2495.
Pallier C, Sebastian-Gallés N, Dupoux E, Christophe A, Mehler J (1998) Perceptual adjustment to time-compressed speech: a cross-linguistic study. Mem Cognit 26:844–851.
Pallier C, Devauchelle AD, Dehaene S (2011) Cortical representation of the constituent structure of sentences. Proc Natl Acad Sci U S A 108:2522–2527.
Pashler H (1984) Processing stages in overlapping tasks: evidence for a central bottleneck. J Exp Psychol Hum Percept Perform 10:358–377.
Pashler H (1994) Dual-task interference in simple tasks: data and theory. Psychol Bull 116:220–244.
Peelle JE, McMillan C, Moore P, Grossman M, Wingfield A (2004) Dissociable patterns of brain activity during comprehension of rapid and syntactically complex speech: evidence from fMRI. Brain Lang 91:315–325.
Peelle JE, Troiani V, Wingfield A, Grossman M (2010) Neural processing during older adults' comprehension of spoken sentences: age differences in resource allocation and connectivity. Cereb Cortex 20:773–782.
Poldrack RA, Temple E, Protopapas A, Nagarajan S, Tallal P, Merzenich M, Gabrieli JD (2001) Relations between the neural bases of dynamic auditory processing and phonological processing: evidence from fMRI. J Cogn Neurosci 13:687–697.
Potter M, Kroll JF, Harris C (1980) Comprehension and memory in rapid sequential reading. In: Attention and performance VIII (Nickerson R, ed), pp 395–418. Hillsdale, NJ: Erlbaum.
Raymond JE, Shapiro KL, Arnell KM (1992) Temporary suppression of visual processing in an RSVP task: an attentional blink? J Exp Psychol Hum Percept Perform 18:849–860.
Reynolds ME, Givens J (2001) Presentation rate in comprehension of natural and synthesized speech. Percept Mot Skills 92:958–968.
Rubin GS, Turano K (1992) Reading without saccadic eye movements. Vision Res 32:895–902.
Saur D, Schelter B, Schnell S, Kratochvil D, Küpper H, Kellmeyer P, Kümmerer D, Klöppel S, Glauche V, Lange R, Mader W, Feess D, Timmer J, Weiller C (2010) Combining functional and anatomical connectivity reveals brain networks for auditory language comprehension. Neuroimage 49:3187–3197.
Sebastián-Gallés N, Dupoux E, Costa A, Mehler J (2000) Adaptation to time-compressed speech: phonological determinants. Percept Psychophys 62:834–842.
Sergent C, Dehaene S (2004) Is consciousness a gradual phenomenon? Evidence for an all-or-none bifurcation during the attentional blink. Psychol Sci 15:720–728.
Sigman M, Dehaene S (2008) Brain mechanisms of serial and parallel processing during dual-task performance. J Neurosci 28:7585–7598.
Sigman M, Jobert A, Lebihan D, Dehaene S (2007) Parsing a sequence of brain activations at psychological times using fMRI. Neuroimage 35:655–668.
Sperling G (1960) The information available in brief visual presentation. Psychol Monogr 74:1–29.
Stromswold K, Caplan D, Alpert N, Rauch S (1996) Localization of syntactic comprehension by positron emission tomography. Brain Lang 52:452–473.
Swaab TY, Brown C, Hagoort P (1998) Understanding ambiguous words in sentence contexts: electrophysiological evidence for delayed contextual selection in Broca's aphasia. Neuropsychologia 36:737–761.
ter Keurs M, Brown CM, Hagoort P, Stegeman DF (1999) Electrophysiological manifestations of open- and closed-class words in patients with Broca's aphasia with agrammatic comprehension: an event-related brain potential study. Brain 122:839–854.
ter Keurs M, Brown CM, Hagoort P (2002) Lexical processing of vocabulary class in patients with Broca's aphasia: an event-related brain potential study on agrammatic comprehension. Neuropsychologia 40:1547–1561.
Tyler LK, Marslen-Wilson W (2008) Fronto-temporal brain systems supporting spoken language comprehension. Philos Trans R Soc Lond B Biol Sci 363:1037–1054.
Wassenaar M, Hagoort P (2005) Word-category violations in patients with Broca's aphasia: an ERP study. Brain Lang 92:117–137.
Waters GS, Caplan D (1996) The capacity theory of sentence comprehension: critique of Just and Carpenter (1992). Psychol Rev 103:761–772.
Zylberberg A, Dehaene S, Mindlin GB, Sigman M (2009) Neurophysiological bases of exponential sensory decay and top-down memory retrieval: a model. Front Comput Neurosci 3:4.
Zylberberg A, Fernández Slezak D, Roelfsema PR, Dehaene S, Sigman M (2010) The brain's router: a cortical network model of serial processing in the primate brain. PLoS Comput Biol 6:e1000765.